Electronic properties of a realistic model of amorphous silicon

S. K. Bose, K. Winer, and O. K. Andersen
Max-Planck-Institut für Festkörperforschung, Heisenbergstrasse 1, D-7000 Stuttgart 80, Federal Republic of Germany
(Received 14 August 1987)

We present the results of a first-principles calculation of the electronic density of states for a large, realistic model of amorphous silicon (*a*-Si). The structural basis of the calculation is a 216-atom, fully-fourfold-coordinated model of *a*-Si with periodic boundary conditions, whose pair-correlation function, average geometric distortions, and vibrational properties are in good agreement with experiment. The calculation is carried out by using the recursion method in conjunction with the tight-binding linear muffin-tin orbitals scheme in its simplest form. To assess the accuracy of our results, we apply the method to a crystalline silicon cluster and obtain a density of states similar to that obtained with the conventional Brillouin-zone summation method. The valence-band density of states calculated for the *a*-Si model shows good overall agreement with that measured for *a*-Si by x-ray photoelectron spectroscopy. The Si 3*p* valence-band peak is found to shift by 0.5 eV to lower binding energy compared with its position in the crystal, and the Si 3*s* and "*s*-*p*" hybrid bands of the crystal merge into one broad band in the amorphous model. We examine the local density of states of several atoms in the center of the cluster and the charge content of the corresponding atomic spheres to determine the effects of geometric distortion on the density of states and the degree of local distortion-induced static charge transfer. The rms static charge deviation is 0.14*e*, which is in good agreement with the experimental value of 0.11*e*. We find that neither particular features in the local densities of states nor the charge deviations from the mean of atoms in the center of the *a*-Si unit cell are correlated with the surrounding local geometric or topological distortions. Sharp peaks in the spectral functions of the *a*-Si model indicate remnants of the E-$\mathbf{k}$ dispersion relations for both *s*- and *p*-like states near $\mathbf{k}\approx\mathbf{0}$. The peaks broaden for larger values of $\mathbf{k}$, in agreement with the dispersion behavior in disordered semiconductors suggested by Ziman.

I. INTRODUCTION

Amorphous silicon (*a*-Si), the prototypical disordered semiconductor, has been the subject of an extensive amount of experimental as well as theoretical investigation. Not surprisingly then, the electronic structure of *a*-Si has been studied with a variety of theoretical methods.[1–10] In addition to qualitatively reproducing the experimentally measured electronic density of states,[11–13] theoretical studies have attempted to provide some understanding of the changes in the electronic states caused by disorder. Ziman[1] has argued that a small amount of disorder might considerably effect the top of the valence band, but leave the bottom part unchanged. Weaire[2] and Weaire and Thorpe[3] have shown, based on a simple model Hamiltonian, that an energy gap could persist in the amorphous state as a result of short-range order. Kelly and Bullett,[4] using an extended form of the Weaire-Thorpe Hamiltonian, calculated the electronic density of states for various topologically distinct models of *a*-Si and thus were able to study the effect of the ring structure on the electronic density of states. Joannopoulos and Cohen[6] studied the electronic structure of silicon polymorphs and determined that fivefold rings were responsible for the filling up of the deep minima between the valence-band peaks in *a*-Si. A qualitative study of the effects of various types of disorder (bond-length and angle variations, dihedral angle variations, and the presence of oddfold rings) was carried out by Cohen, Yonezawa, and Singh[7–9] using model tight-binding Hamiltonians. Singh[9] found the effects of topological and dihedral angle disorder to be the most pronounced. Joannopoulos,[10] in an earlier study using the cluster–Bethe-lattice method and nearest-neighbor interactions, found bond-angle disorder to be more important than bond-length disorder in determining the electronic structure of the clusters.

Although much is known concerning the nature of the electronic states in disordered tetrahedrally bonded semiconductors, calculations of the electronic properties of amorphous silicon based on large, realistic structural models and accurate first-principles Hamiltonians are still needed. The qualitative effects of disorder that have been examined on the basis of model Hamiltonians can then be quantified and studied in more detail. In this paper we calculate the electronic properties of a recently constructed fully fourfold-coordinated 216-atom periodic model of *a*-Si.[14] This is the largest amorphous silicon model available at present whose structural and vibrational properties have been fully characterized[15] and found to be in good agreement with the latest experimental information. As such, the model should be a reasonable representation of the bulk, homogeneous structure of *a*-Si, which warrants the study of its electronic properties. Hickey and Morgan[16] have recently calculated the electronic density of states and spectral functions for a

similar 216-atom periodic structure using a model pseudopotential and the equation of motion method in **k** space. Our study, like that of Kelly and Bullett,[7] is based on a real-space approach (recursion method),[17] where it is easy to calculate the electronic density of states projected onto various atoms in the cluster. This enables us to study the effects of the local environment on the electronic states. Also, we have used a scheme for calculating the one-electron Hamiltonian which is different from that used by Hickey and Morgan.[16]

The one-electron Hamiltonian used in our calculation has been derived using the tight-binding linear muffin-tin orbitals (TB LMTO) scheme in its simplest form.[18,19] This uses the atomic-sphere approximation (ASA),[19] and the one-electron Hamiltonian is correct to first order in deviations from some reference energy E_ν. This Hamiltonian has the two-center tight-binding form and is expressed in terms of potential parameters and a hopping matrix that depends only on the structure. The potential parameters are local quantities, obtained from the solution of the one-electron wave equation at the energy E_ν inside the atomic or Wigner-Seitz sphere surrounding the atom. We expect that in the transition from the crystalline to the amorphous phase, the spherical part of the potential inside a given sphere should change only slightly; the corresponding potential parameters should remain virtually unchanged. Changes in the electronic structure should then arise primarily from changes in the hopping matrix, and the potential parameters can be treated as transferable quantities. However, the scheme does not necessarily rely on their tranferability. The potential parameters can be calculated for any system with a reasonable starting guess for the potential inside the spheres and recalculated in an iterative manner until self-consistency in the charge distribution is achieved.[19] Thus the TB LMTO formalism provides a scheme for a first-principles self-consistent electronic-structure calculation, and can also be used as a semiempirical tight-binding scheme under suitable conditions. The TB LMTO scheme is relatively new and, as far as electronic-structure calculations for amorphous systems are concerned, it has so far been applied only to the study of amorphous Fe and some binary amorphous alloys.[20,21] The present calculation is the first application of the method to an open amorphous structure.

The remainder of this paper is divided into sections as follows. In the next section we outline the TB LMTO method. In Sec. III we present results for crystalline silicon in the diamond structure (c-Si). We calculate the band structure and the electronic density of states. We compare the density of states calculated by using the conventional Brillouin-zone summation method and the recursion method. This gives us an estimate of the loss of accuracy in the recursion method stemming from the termination of the continued-fraction expansion of the Green's function as well as the finite cluster size. In Sec. IV we present the results for the a-Si model including both the valence- and conduction-band densities of states. A comparison of our results with other theoretical calculations and with experiment is made. We also attempt to relate features of the electronic density of states to local environments in the cluster. In Sec. V we discuss the limitations of the present calculation and indicate how improvements might be made.

II. THE TB LMTO METHOD

In this section we describe how the TB LMTO's are related to the standard solid-state LMTO's (Ref. 22) and outline the main results of the TB LMTO scheme used here. For proofs and further details, we refer to Refs. 19, 23, and 24. The application of TB LMTO's to amorphous systems is discussed in Ref. 21.

In the LMTO method space is divided into muffin-tin spheres centered at various atomic and possibly interstitial sites **R**, and the interstitial region. The potential inside the spheres is assumed to be spherically symmetric, while outside the spheres it is assumed to be constant. The potential is calculated using the local-density approximation to the exchange-correlation potential in the density-functional theory of Hohenberg and Kohn.[22] The basis set in the conventional or unscreened LMTO method consists of functions $\chi^0_{RL}(\mathbf{r}-\mathbf{R})$ centered about the sites **R** in the solid, where L ($\equiv\{l,m\}$) is the (collective) angular-momentum index and

$$\chi^0_{RL}(\mathbf{r}-\mathbf{R})=K^0_{RL}(\mathbf{r}-\mathbf{R})+\Phi_{RL}(\mathbf{r}-\mathbf{R}) + \sum_{R',L'} \dot{\Phi}^0_{R'L'}(\mathbf{r}-\mathbf{R}')h^0_{R'L'RL} \ . \quad (1)$$

Here, K^0_{RL} is the envelope function which is supposed to vanish inside all the spheres, while in the interstitial region it is given by the solution of the one-electron Schrödinger equation with the electron energy equal to the muffin-tin zero of the potential. The choice of the electron energy equal to the muffin-tin zero reduces the Schrödinger equation to the Laplace equation in the interstitial region. K^0_{RL} is thus taken to be proportional to

$$|\mathbf{r}-\mathbf{R}|^{-l-1}Y_L(\theta,\varphi) \ ,$$

the solution of the Laplace equation that is irregular at **R** but regular at infinity. It is the field of a 2^l pole situated at the site **R**. The functions Φ_{RL} and $\dot{\Phi}_{RL}$ are supposed to vanish outside the sphere at **R**. Φ_{Rl} is the normalized solution of the radial part of the wave equation for orbital angular momentum l inside the sphere at **R** for reference energy $E_{\nu Rl}$, and $\dot{\Phi}^0_{Rl}$ is a linear combination of Φ_{Rl} and its energy derivative $\dot{\Phi}_{Rl}$ at the energy $E_{\nu Rl}$. These linear combinations and the quantities $h^0_{R'L'RL}$ in Eq. (1) are chosen to ensure the continuity and differentiability of χ^0_{RL} at the surfaces of all the spheres. They contain information concerning the atomic positions **R** and **R'**, as well as the phi and phi-dot functions at the boundaries of the spheres centered at these positions.

The coefficients $h^0_{R'L'RL}$ depend on the sphere positions through the bare canonical structure constants $S^0_{R'L'RL}$, which do not depend on the sphere types or radii. The on-site elements of $S^0_{RLR'L'}$, $S^0_{RLRL'}$ are zero, and the expression for $S^0_{RLR'L'}$ for arbitrary **R** and **R'** is discussed in Refs. 19 and 25. The structure constants $S^0_{RLR'L'}$ contain long-range components. As a function of the separation $d=|\mathbf{R}-\mathbf{R}'|$, they behave as

$$S^0_{RLR'L'}\sim(w/d)^{l+l'+1} \ . \quad (2)$$

The matrix elements of the one-electron Hamiltonian, which can be shown to be directly related to the coefficients $h^0_{RLR'L'}$, and thus to $S^0_{RLR'L'}$, are also long ranged. The long range of these matrix elements poses no problems in the electronic-structure calculation for crystalline systems where one can use the Ewald technique to evaluate the Bloch sum. For calculations involving systems where the periodicity is either missing or broken, one must use a real-space method such as the moment[26] or the recursion[17] methods, which rely on having well-localized basis orbitals. The matrix elements of $\underline{H}$, more precisely of $\underline{O}^{-1}\underline{H}$ or $\underline{O}^{-1/2}\underline{H}\,\underline{O}^{-1/2}$ (where $\underline{O}$ is the overlap), must decay rapidly with interatomic separation. Within the LMTO formalism this rapid decay with increasing interatomic distance is achieved by changing the envelope function of the basis orbitals in Eq. (1). In the TB LMTO method one uses envelope functions K^α_{RL} which are similar to K^0_{RL} in the neighborhood of $\mathbf{R}$, but are screened by multipoles situated at the neighboring atoms. This gives rise to the screened structure matrix $\underline{S}^\alpha$ in the theory, which is related to the bare structure matrix via the relation

$$\underline{S}^\alpha=\underline{S}^0(\underline{1}-\underline{\alpha}\,\underline{S}^0)^{-1} \quad \text{or} \quad \underline{S}^\alpha=\underline{S}^0+\underline{S}^0\underline{\alpha}\,\underline{S}^\alpha \ . \tag{3}$$

As discussed by Andersen and co-workers[21,23,27] different choices for the screening matrix $\underline{\alpha}$ lead to basis sets with different properties, constituting different LMTO representations. In the TB LMTO representation used in this work, $\underline{\alpha}$ is supposed to be a site-independent, but l-dependent, matrix with only three nonzero elements:

$$\alpha_l=\begin{cases}0.3485 & \text{for } l=0\ ,\\ 0.05303 & \text{for } l=1\ ,\\ 0.010714 & \text{for } l=2\ ,\\ 0 & \text{for } l\geq 3\ .\end{cases} \tag{4}$$

It has been found that with nonzero screening on all sites in the solid for $l=0$, 1, and 2, these α values give rise to the most localized LMTO basis orbitals and short-ranged structure matrix elements for all reasonably homogeneous structures. Beyond the second-neighbor shell the screening is practically complete in the α-LMTO representation. Other choices are possible and are still being studied.[23,27]

$\underline{S}^\alpha$, like $\underline{S}^0$, involves a length parameter w. Although in $\underline{S}^0$ the choice of w is somewhat arbitrary and basically fixes the unit of length, in $\underline{S}^\alpha$ the choice of w must be consistent with that of the screening parameters. It depends on the concentration of the screening multipoles and must be calculated from the volume V_0 per site through the relation

$$V_0=(4\pi/3)w^3\ . \tag{5}$$

In the TB or α representation the LMTO basis orbitals are linear combinations of the conventional orbitals [Eq. (1)], and the TB LMTO centered at $\mathbf{R}$ is given by an expression similar to Eq. (1):

$$\chi^\alpha_{RL}(\mathbf{r}-\mathbf{R})=K^\alpha_{RL}(\mathbf{r}-\mathbf{R})+\Phi_{RL}(\mathbf{r}-\mathbf{R}) + \sum_{R',L'}\dot{\Phi}^\alpha_{R'L'}(\mathbf{r}-\mathbf{R}')h^\alpha_{R'L'RL}\ . \tag{6}$$

As in Eq. (1), we consider K^α_{RL} to be nonzero only in the interstitial region and to be augmented by linear combinations of Φ and $\dot{\Phi}^\alpha$ functions inside the spheres. The latter are given by

$$\dot{\Phi}^\alpha_{Rl}(r)=\dot{\Phi}_{Rl}(r)+\Phi_{Rl}(r)o^\alpha_{Rl}\ , \tag{7}$$

$$\dot{\Phi}_{Rl}(r)=\left.\frac{\partial\Phi_{Rl}(E,r)}{\partial E}\right|_{E=E_{\nu Rl}}\ . \tag{8}$$

The coefficients o^α are determined to give $\dot{\Phi}^\alpha$ the same radial logarithmic derivative at the sphere radius as the tail of the envelope function K^α. The multiplication by h^α in Eq. (6), finally, makes the augmentation continuous at the sphere boundary. The coefficients h^α have the form[23,24]

$$h^\alpha_{RLR'L'}=(c^\alpha_{Rl}-E_{\nu Rl})\delta_{RR'}\delta_{LL'} +(d^\alpha_{Rl})^{1/2}S^\alpha_{RLR'L'}(d^\alpha_{R'l'})^{1/2}\ , \tag{9}$$

where c^α_{Rl} and d^α_{Rl} are potential parameters which may be found from the value and slope of $\Phi_{Rl}(r)$ at the sphere boundary (see Appendix).

A frequently used approximation in the LMTO method is the atomic-sphere approximation (ASA), in which one replaces the muffin-tin spheres with Wigner-Seitz spheres and neglects the remaining interstitial region. This is possible for closely packed materials, as well as for those open structures which can be close packed with the addition of interstitial ("empty") spheres. The diamond structure, for example, can be packed like a bcc lattice with the addition of interstitial spheres. In the calculation for crystalline silicon we thus have spheres situated at both atomic and interstitial sites, to be referred to as the silicon spheres and empty spheres, respectively. Both silicon and empty spheres may have TB LMTO's χ^α_{RL} and screening charges α_{Rl} associated with them, with l varying from 0 to 2. Putting empty spheres in an amorphous silicon structure is a nontrivial problem and will be discussed in Sec. IV, where the results for amorphous silicon are presented.

In the expression for the TB LMTO in the ASA the first term on the right-hand side (rhs) of Eq. (6) drops out. The Hamiltonian and the overlap matrices receive no contribution from the interstitial region and are given by[19,23,24]

$$\underline{H}=\underline{h}+\underline{h}\,\underline{o}\,\underline{h}+(\underline{I}+\underline{h}\,\underline{o})\underline{E}_\nu(\underline{I}+\underline{o}\,\underline{h})+\underline{h}\,\underline{p}\,\underline{E}_\nu\,\underline{h} \tag{10}$$

and

$$\underline{O}=\langle\chi\,|\,\chi\rangle=(\underline{I}+\underline{h}\,\underline{o})(\underline{I}+\underline{o}\,\underline{h})+\underline{h}\,\underline{p}\,\underline{h}\ . \tag{11}$$

In Eqs. (10) and (11) we have dropped the superscripts α implying the TB representation. $\underline{h}$ and $\underline{o}$ are the matrices appearing in Eqs. (6) and (7), $\underline{o}$ is diagonal, $\underline{I}$ is the unit matrix, and $\underline{p}$ is a diagonal matrix with elements

$$p_{Rl}=\int\dot{\Phi}^2_{Rl}(r)r^2\,dr\ , \tag{12}$$

where the integration is performed within the atomic sphere at $\mathbf{R}$. The p_{Rl}'s are small parameters and a reasonable approximation to $\underline{O}$ can be obtained by dropping the last term on the rhs of Eqs. (10) and (11). Be-

cause of the finite overlap $\underline{O}$, the eigenvalue equation to be solved is either

$$\det | \underline{O}^{-1}\underline{H} - E\underline{I} | = 0$$

or (13)

$$\det | \underline{O}^{-1/2}\underline{H}\,\underline{O}^{-1/2} - E\underline{I} | = 0 \ .$$

In using the recursion method[17] it is easier to consider the latter form, because it involves the tridiagonalization of a symmetric matrix. With the neglect of the small quantities p_{Rl}, the Löwdin-orthonormalized Hamiltonian in the ASA (Refs. 19 and 23) assumes the form

$$\underline{H}^{(2)} = \underline{O}^{-1/2}\underline{H}\,\underline{O}^{-1/2} = \underline{E}_\nu + \underline{h}(\underline{I} + \underline{o}\,\underline{h})^{-1} \quad (14a)$$

$$= \underline{E}_\nu + \underline{h} - \underline{h}\,\underline{o}\,\underline{h} + \cdots \ . \quad (14b)$$

Thus in the ASA the Hamiltonian to be considered, correct to first order in deviations from the reference energies E_ν, is simply

$$\underline{H}^{(1)} = \underline{E}_\nu + \underline{h} \ , \quad (15)$$

with the matrix $\underline{h}$ given by Eq. (9). The corresponding second-order Hamiltonian is $H^{(2)}$ [Eq. (14b)].

The calculation of electronic structure using the TB LMTO method thus involves two steps: (1) calculating the potential parameters c^α_{Rl}, d^α_{Rl}, and o^α_{Rl} (see Appendix), and (2) calculating the screened structure matrix $S^\alpha_{RLR'L'}$. The screened structure matrix $\underline{S}^\alpha$ can be calculated from the unscreened structure matrix $\underline{S}^0$, which can be expressed analytically,[19,25] either by iterating the Dyson equation (3) to self-consistency, or through the matrix inversion given in Eq. (3).[28] The off-site elements of the tight-binding structure matrix $\underline{S}^\alpha$ can also be obtained from an interpolation formula valid for the Slater-Koster "hopping integrals" $\bar{S}_{ll'm}(d)$,[19,23] where the intersite vector is along the z axis. The interpolation formula that holds extremely well for all cubic structures is of the form

$$\bar{S}_{ll'm}(d) = S_{ll'm} \exp(-z^{q_{ll'm}}/z^{p_{ll'm}}), \quad z = \lambda_{ll'm} d/w \quad (16)$$

where the values of p, q, S, and λ for various "hopping integrals" $ss\sigma$, $sp\sigma$, . . . are given in Table II of Ref. 19. Another interpolation formula, somewhat less accurate than Eq. (16) for cubic structures, but better in general for an arbitrary structure, is of the form

$$\bar{S}_{ll'm}(d) = S_{ll'm} e^{-z}, \quad z = \lambda_{ll'm} d/w \quad (17)$$

and the values of S and λ are available in Table II of Ref. 23 and in Table I of Ref. 24. The on-site elements of the tight-binding structure matrix are nonzero and depend on the local environment. There is no simple interpolation formula for these, but they can be calculated using the off-site elements of $\underline{S}^\alpha$ in the Dyson equation

$$S^\alpha_{RLRL'} = \sum_{\substack{R'',L'' \\ (R''\neq R)}} S^\alpha_{RLR''L''}\alpha_{R''L''}S^0_{R''L''RL'} \ . \quad (18)$$

In a self-consistent LMTO calculation involving the Hamiltonian and overlap matrices (10) and (11), only one set of $E_{\nu Rl}$'s, chosen to lie at the center of gravity of the occupied part of the Rl-projected band, is often used.[19] This choice results in accurate valence-band energies and hence accurate charge distributions in the various spheres. However, use of merely the first-order approximation (15) makes it necessary to perform several calculations involving more than one set of $E_{\nu Rl}$'s, so that accurate results are obtained over a wide range of energies. In crystalline structures the potential parameters depend on the types of the spheres but not on their positions. In amorphous structures the potential parameters should, in principle, depend on the positions of the spheres as well. However, in the present calculation we have considered them to depend on the sphere type only. Although we have not performed a self-consistent calculation, the potential parameters for both the c-Si and a-Si clusters were calculated using the potentials in the silicon and empty spheres obtained from a self-consistent unscreened LMTO calculation for c-Si.[29] Two sets of $E_{\nu l}$'s were used in the calculation, one to produce accurate results in the center of the valence band, and the other for the near-gap part of the conduction band. As in the self-consistent case, our choice of the former provides the best estimate for the valence-band energies and hence the best estimate for the valence charge distribution.

III. RESULTS FOR SILICON IN THE DIAMOND STRUCTURE

In the calculation for c-Si, empty spheres are placed at the tetrahedral holes, i.e., the positions $(\frac{1}{2},\frac{1}{2},\frac{1}{2})a_0$ with respect to the silicon lattice sites, where $a_0 = 5.4271$ Å is the lattice parameter for the diamond structure. This generates a bcc structure, for which the interpolation formula [Eq. (16)] for the off-site elements of the screened structure matrix yields values almost identical to those obtained via matrix inversion. Hence we use Eq. (18) in conjunction with Eq. (16) to calculate the screened structure matrix with $l = 0$, 1, and 2 orbitals for both the silicon atoms and the empty spheres. The potentials in the silicon and empty spheres were taken from a self-consistent "scalar-relativistic" standard (unscreened) LMTO calculation by Christensen,[29] who used equal sphere sizes ($s_{\rm Si} = s_E = 1.336$ Å) and the local-density approximation for exchange and correlation. From this potential we calculate the potential parameters c^α, d^α, and o^α for $l = 0$, 1, and 2 in the silicon and empty spheres. The energies $E_{\nu l}$ for the silicon and the empty spheres, obtained from the calculation of Ref. 29, are at the centers of gravity of the occupied part of the respective l bands (see Table I). The first-order two-center tight-binding Hamiltonian $H^{(1)}$ [Eqs. (9) and (15)] calculated with these parameters will be referred to as $H^{(1)}_1$. In Figs. 1(a) and 1(b) we show, for $H^{(1)}_1$, both the band structure and the density of states obtained via Brillouin-zone summation using the linear tetrahedron scheme of Jepsen and Andersen.[30] The spectrum has no gap and it is compressed in the conduction-band region. For E_ν in the valence band, the Si s and p overlap parameters σ^α are negative (see Table I). $H^{(1)}_1$ lacks the second-order correction $-(E-E_\nu)^2\sigma^\alpha$ [see Eq. (14b)] which pushes the eigenvalues far from E_ν towards higher energy. Thus using $H^{(1)}_1$ with E_ν's in the valence band leads to an in-

correctly large density of states in the conduction band. To obtain better results one can consider the Hamiltonian $H^{(2)}$ [Eq. (14a)] for the same E_ν's used in $H_1^{(1)}$.[31] The band structure and the density of states for $H^{(2)}$, with the same E_ν's as in $H_1^{(1)}$, are shown in Figs. 1(c) and 1(d). A small gap of width ~ 0.5 eV opens up, and both the valence and conduction bands are in better agreement with the results of the standard third-order LMTO calculation which uses Eqs. (10) and (11) (Fig. 7 of Ref. 29).

For amorphous clusters involving ~ 4000 orbitals, such as the one considered here, the calculation of $H^{(2)}$ is somewhat time consuming and we have consequently only carried out the calculations using $H^{(1)}$. It is, however, necessary to perform at least a two-panel calculation; one must use two sets of E_ν's. In order to treat the gap region and the bottom part of the conduction band properly, we set all E_ν's equal to an energy (zero) close to the bottom of the conduction band. This calculation then yields a gap of ~ 0.5 eV. Also, we make a small departure from a "first-principles" calculation in an attempt to increase the size of the gap. The widths of the energy gaps in semiconductors obtained by using the Kohn-Sham density-functional theory in its local approximation are typically only half of the experimentally measured values of 1.1 eV.[32] Somewhat empirically, we can widen the gap by shifting the c_{RL}^{α} parameters for the s orbitals upward in energy relative to those of the p orbitals.[33] For small shifts this primarily effects the bottoms of the valence and conduction bands, the Γ_1 and X_1 points, leaving other parts of the band unchanged. In Figs. 1(e) and 1(f) we show the band structure and density of states for the Hamiltonian $H_2^{(1)}$, where the E_ν's are the same as in $H_1^{(1)}$, but the c_{RL}^{α} parameters for the s states on the silicon and empty spheres have been moved up in energy by 0.1 Ry. The gap turns out to be close to that obtained with $H^{(2)}$ without the gap correction, and the valence band is in good agreement with the standard LMTO results[29] as well as with experiment.[3] In order to describe the conduction band properly, we repeat the calculation following the same procedure, but with all the E_ν's set equal to zero. We refer to the resulting Hamiltonian as $H_3^{(1)}$. The band structure and the density of states for this case are shown in Figs. 1(g) and 1(h). The resulting energy gap agrees well with the experimental value of 1.1 eV. The bottom of the valence band is too low because o^{α} for the Si and E s orbitals are negative and the prefactor $(E-E_\nu)^2$ is of order 1 Ry^2. The potential parameters for the Hamiltonians $H_2^{(1)}$ and $H_3^{(1)}$ are given in Tables I and II, respectively. For $H_1^{(1)}$ all parameters remain the same as in Table I except the c parameters, which do not have the additional 0.1-Ry shift.

The accuracy of the results using the recursion method[17] depend mainly on two factors, the cluster size and the terminator for the continued fraction. The cluster size determines the number of recursion coefficients that can be calculated without error, i.e., without any interference from the cluster surface. The terminator[34,35] attaches a tail of coefficients to the calculated values in order to simulate the result of an infinite system. We have used the "linear predictor terminator" proposed by Allan.[35] The calculated coefficients are fitted to a complex Fourier series, which is then used to extrapolate 300–500 coefficients. All of these coefficients, together with the constant chain terminator,[17] are used in the expression for the diagonal matrix element of the Green's function. The "linear predictor terminator" has been shown to yield good results for c-Si when applied to approximately 20 exactly calculated coefficients.[35] It has also been tested, with good results, for various model densities of states with multiple gaps and band-edge singularities, where the continued-fraction coefficients were calculated from the moments of the assumed distributions.[36]

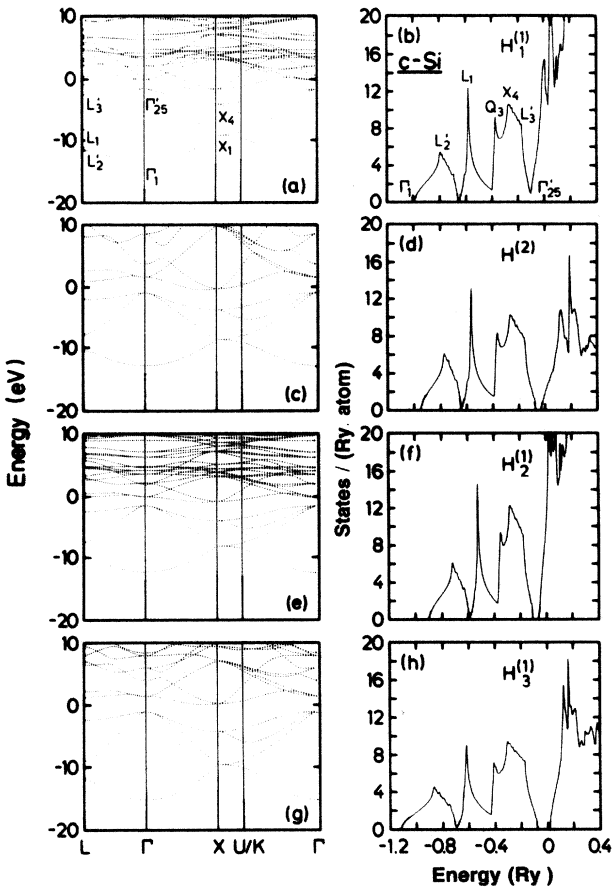

FIG. 1. Band structure and density of states of c-Si obtained by using the LMTO Hamiltonians $H_1^{(1)}$, $H^{(2)}$, $H_2^{(1)}$, and $H_3^{(1)}$ described in the text. The $H^{(1)}$'s are first-order two-center tight-binding Hamiltonians and $H^{(2)}$ is the Hamiltonian in the nearly orthogonal representation. The eigenvalues of $H^{(2)}$ are the one-electron energies correct to second order. For $H_1^{(1)}$, $H^{(2)}$, and $H_2^{(1)}$ the E_ν's are chosen in the valence band, and for $H_3^{(1)}$ they are chosen in the gap. $H_2^{(1)}$ and $H_3^{(1)}$ contain a correction for the error of the local-density approximation as described in the text.

It is important to assess the effects of cluster size and the boundary conditions (e.g., periodic or free) on the results obtained with the recursion method.[37] We find that for a crystalline cluster of 432 sites (216 silicon and 216 empty spheres) the density of states obtained by using the recursion method together with periodic boundary conditions shows fair agreement with that calculated by the

TABLE I. Potential parameters for Hamiltonian $H_2^{(1)}$ (the shift in the c parameter for the s orbitals, used to widen the gap, is shown explicitly, and the superscript α has been dropped).

	l	E_v (Ry)	c (Ry)	$d^{1/2}$ (Ry$^{1/2}$)	o (Ry^{-1})
Silicon	0	−0.6574	−0.8829+0.1	0.4269	−0.3195
Spheres	1	−0.3083	0.0350	−0.3159	−0.3764
	2	−0.3227	0.5290	0.1764	−0.6217
Empty	0	−0.4987	−0.0811+0.1	0.3287	−0.5397
Spheres	1	−0.4205	0.3482	0.2036	−0.7086
	2	−0.3487	0.3194	0.0925	−1.2074

more exact Brillouin-zone–summation scheme. However, the minima between the three main peaks are rather shallow and the gap between the valence and conduction bands appears only as a minimum in the density of states. Increasing the cluster size makes these minima more pronounced and, in general, sharpens the features in the c-Si density of states. We have found that to obtain a density of states with the recursion method in acceptable agreement with the more exact result (see Fig. 2), we must extend the cluster size to at least 800 sites (400 Si atoms),[38] if free boundary conditions are used. In Figs. 2(a) and 2(b) we show a comparison of the recursion method results with the Brillouin-zone–summation calculation for the density of states of c-Si using the Hamiltonians $H_2^{(1)}$ and $H_3^{(1)}$. The recursion calculations were performed for crystalline clusters with ~855 sites using free boundary conditions. Five-hundred coefficients were extrapolated, typically from nine s, seventeen p, and twenty d calculated values, using the "linear predictor" method. Even for a cluster this large we found that only the first six or seven s and nine to fifteen p coefficients could be calculated exactly for atoms in the center of the cluster. Higher coefficients begin to accumulate errors that increase with the length of the chain. This is the reason why even with the "linear predictor terminator" we do not obtain a well-defined gap, although qualitative agreement with the more exact Brillouin-zone–summation calculation is good.

The position of the peaks associated with the critical points L_2' and L_1 are reproduced well by the recursion method.[39] However, the minima following these peaks are shallower than those produced by the **k**-space calculation. Also, the peaks associated with the critical points Q_3 (Ref. 39) and X_4 are moved towards higher energies and the weak singularity at L_3' is washed out. All of these results can be understood in terms of the loss of information about the crystal structure in the recursion-method calculation away from the central region of the cluster. Because some of the higher calculated recursion coefficients (or moments), and the extrapolated ones as well, are somewhat in error, the structure "seen" by the recursion method becomes increasingly disordered. This results in the shift of the p-band peaks towards higher energy and the filling up of the minima following the L_2' and L_1 peaks. These deviations from the c-Si electronic density of states obtained by Brillouin-zone summation should become even more pronounced for our a-Si model because of its relatively large structural distortions.

Comparison of the recursion-method results with those obtained by Brillouin-zone summation gives us an estimate of the accuracy of our calculations (see Fig. 2). Because with the recursion method we are able to reproduce fairly well the main features in the density of states for a c-Si cluster of 855 sites (except the gap region), we should be able to apply the method to an a-Si cluster of similar size and obtain the same degree of accuracy. In fact, we expect the error to be larger in the crystalline case, because in order to reproduce the sharp features in the corresponding density of states, a larger number of correct moments is needed. Therefore we expect the recursion method to provide a good description of the density of states for the amorphous structure in almost the entire energy region of interest, except the gap.

IV. RESULTS FOR THE AMORPHOUS SILICON MODEL

The differences in the electronic or other properties of crystalline as compared to amorphous silicon stem direct-

TABLE II. Potential parameters for Hamiltonian $H_3^{(1)}$ (the shift in the c parameters for the s orbitals, used to widen the gap, is shown explicitly, and the superscript α has been dropped).

	l	E_v (Ry)	c (Ry)	$d^{1/2}$ (Ry$^{1/2}$)	o (Ry^{-1})
Silicon	0	0.0	−1.0214+0.1	0.4856	−0.0657
Spheres	1	0.0	0.0804	−0.3498	−0.2836
	2	0.0	0.8342	0.2107	−0.4939
Empty	0	0.0	0.0300+0.1	0.4079	−0.3300
Spheres	1	0.0	0.7416	0.2632	−0.5264
	2	0.0	0.8517	0.1314	−0.8443

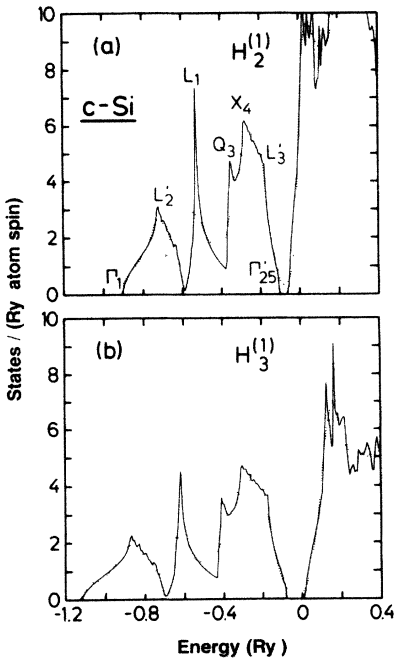

FIG. 2. Comparison of the density of states of c-Si obtained by the Brillouin-zone–summation method (solid line) and the recursion method (dotted line) applied to the TB LMTO Hamiltonians (a) $H_2^{(1)}$ and (b) $H_3^{(1)}$. $H_2^{(1)}$ yields reliable results for the valence-band density of states, while $H_3^{(1)}$ is most reliable near the gap and the bottom part of the conduction band.

ly from the geometric and topological deviations from perfect tetrahedral bonding that characterize the latter phase. Calculated electronic properties will therefore depend to a large extent on the particular structural model one chooses to study. Ideally, one would like a model with several hundred atoms, that is computer generated to eliminate bias, with periodic boundaries for computational convenience and to remove surface effects, and whose pair-correlation function is (and implicitly whose average geometric distortions are) in good agreement with experiment. Although modeling amorphous semiconductor structures has reached a relatively mature stage, the use of divergent model construction criteria is unfortunately still the rule. Therefore it is worthwhile to briefly examine how the model under study was constructed and how well its structural properties agree with those of experiment.

A. Outline of model construction

Model construction starts with a periodic cubic unit cell containing 216 silicon atoms in the perfect diamond structure. We introduce simple topological excitations (pairs of bond switches) (Ref. 14) into the crystal at random and relax the structure after each topological change to its minimum-energy configuration with the Keating potential.[40] We repeat this process until the pair-correlation function of the structure has lost all features characteristic of the diamond structure. The pair-correlation function of such a randomized "crystal" contains broad peaks centered at the first- and second-nearest-neighbor distances of the diamond structure and is slowly varying beyond. This shows that the mean bond length and bond angle are close to their diamond-structure values, but that the "crystal" contains large geometric distortions; the rms bond-length (Δr) and bond-angle ($\Delta\theta$) deviations are typically 3% and 20°, respectively. In order to reduce these distortions, we require that further topological excitations reduce the total Keating potential energy. This reduces the average geometric distortions, but the pair-correlation functions of such structures remain in poor agreement with that of experiment. We reduce the geometric distortions still further by allowing topological excitations that increase the total Keating potential energy. However, such bond switch pairs are accepted only when the thermodynamic probability (through a Maxwell-Boltzmann factor) is greater than some random number between 0 and 1. Such a pseudo–Monte Carlo method (modified Metropolis algorithm) (Ref. 41) allows the structures to tunnel out of highly distorted metastable states and results in structures whose geometric distortions ($\Delta r = 2.2\%$, $\Delta\theta = 11.3°$ for the present model) (Ref. 15) are near to those in real a-Si. The pair-correlation functions of the final structures are also in good agreement with that of experiment.[14,15] The fact that each atom in the present model is a member of at least one oddfold ring[15] means that the topological environment of each atom is different from that of the diamond structure (i.e., the model is purely amorphous). At the same time the exhaustive nature of the model-construction algorithm ensures that the local separation from the diamond structure will be small and roughly the same for all atoms. Because of this homogeneity, the low geometric distortions, the reasonably good agreement with the experimental pair-correlation function, and the lack of local diamond structure, we expect such models to be good approximations to the bulk, homogeneous structure of a-Si. The fact that the vibrational properties of the present model, as well as its structural features, are in good agreement with those of experiment[15] is a good indication that the structural basis we have chosen to calculate the electronic properties of a-Si is a fairly realistic one.

In order to carry out the electronic calculations for the 216-atom a-Si structural model within the TB LMTO scheme, we first need to know the positions of the 216 empty spheres. To start with, we place the empty spheres at sites corresponding to their interstitial positions in the same-size diamond-structure unit cell. The positions of the silicon spheres are taken to be the equilibrium coordinates, relaxed to their minimum-energy configuration with Weber's bond-charge interactions,[42,43] of the model discussed above and in more detail elsewhere.[15] We assume a pair potential with a steep repulsive part (6-16 form) between the spheres, irrespective of their type. The minimum in the potential is chosen to be 2.35 Å, the nearest-neighbor distance in diamond-structure silicon. The potential is terminated at a distance between the first- and second-nearest-neighbor separation in the diamond structure. The empty spheres are moved, keeping the silicon spheres fixed, in order to minimize the energy

of interaction according to the same modified Metropolis algorithm[41] used in the final stages of model construction. The temperature was chosen to be zero for most of the runs. Occasionally we increased the temperature to check whether lower-energy configurations for the empty spheres could be accessed via thermal agitation. The position of the minimum and the cutoff distance in the potential were given small variations in order to minimize the overlap of the spheres inside the fixed cubic volume. When the empty spheres seemed to be stuck in a metastable configuration, we began a new run. The configuration with the minimum overlap between the spheres was finally selected for the electronic-structure calculation. We extended the resultant unit cell of 432 (silicon and empty) spheres periodically and selected a cluster of ~ 1586 spheres from this extended structure. The local densities of states of atoms in the center of this cluster with free boundaries did not differ significantly from those obtained using the original, smaller unit cell of 432 spheres with periodic boundaries. Thus, in contrast to the c-Si calculation, no appreciable change in the density of states was observed by increasing the cluster size. All further results presented for the a-Si model were calculated for the 432-sphere unit cell using periodic boundary conditions.

Calculations for the amorphous cluster were performed using the first-order, two-center, tight-binding Hamiltonians $H_2^{(1)}$ and $H_3^{(1)}$ described in Sec. III. The screened structure matrix was calculated using the interpolation formula (17) for the off-site and (18) for the one-site terms. The average Wigner-Seitz radius w entering the structure matrix was the same as that in c-Si because the a-Si model has the same density as c-Si. We have chosen the potential parameters for both the silicon and empty spheres to be the same as in the calculation for the c-Si cluster. In principle, one should choose sphere radii in an amorphous structure according to the local environment, and the potential parameters should be calculated separately for each sphere. We settle for the computationally feasible approximation of using a single value for all spheres. In view of the fact that we expect the major changes in the electronic structure to result from changes in the structure matrix, this approximation seems reasonable.

B. Average electronic properties

In Figs. 3 and 4 we show a comparison of the density of states for c-Si and a-Si obtained by applying the recursion method to the Hamiltonians $H_2^{(1)}$ and $H_3^{(1)}$. Figures 3(a) and 3(b) are the results for the c-Si and a-Si clusters, respectively, for $H_2^{(1)}$. For this Hamiltonian the reference energies E_v are approximately at the centers of gravity of the occupied part of the Rl-projected bands (see Table I). Hence the valence-band density of states is fairly reliable, while the conduction band is less so. In Figs. 4(a) and 4(b) we show similar results for the Hamiltonian $H_3^{(1)}$, where the E_v's are chosen to be zero (see Table II). In this case the conduction band should be the most reliable, with the results becoming increasingly less accurate towards the bottom of the valence band.

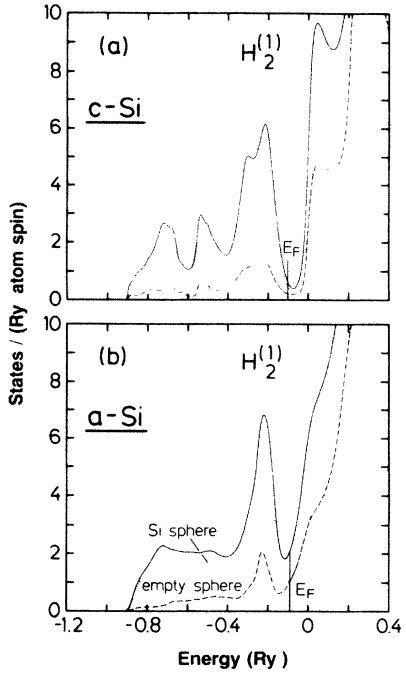

FIG. 3. Density of states of (a) c-Si and (b) a-Si obtained by applying the recursion method to the Hamiltonian $H_2^{(1)}$, which yields reliable results for the valence band. The a-Si density of states was obtained as an average over the densities of states projected onto 40 silicon and 40 empty spheres in the central region of the a-Si cluster. The dotted and dashed lines are the densities of states projected onto the silicon and empty spheres, respectively, in the diamond structure, or their average in a-Si. The solid line is the sum of these two projected densities of states.

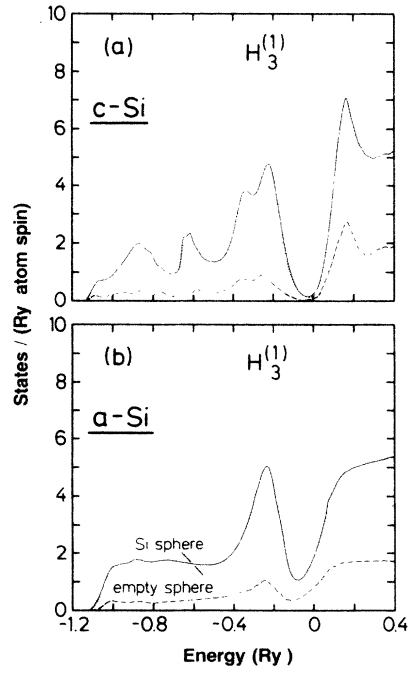

FIG. 4. Same as Fig. 3, but using the Hamiltonian $H_3^{(1)}$, which provides reliable results near the gap and the bottom part of the conduction band.

The densities of states for the amorphous cluster shown in Figs. 3 and 4 are an average over the local densities of states calculated for 40 silicon spheres and 40 empty spheres chosen near the center of the cluster. Each local density of states is a sum over the density of states projected onto the nine orbitals for the corresponding sphere. The dotted curve is the average density of states projected onto the silicon spheres. The most noticeable change in the electronic density of states caused by disorder is the disappearance of the *sp*-bonding peak associated with the critical point L_1. This is apparent not only in the total density of states (solid curve), but also in the density of states projected onto silicon and empty spheres separately. The small peak associated with the critical point Q_3 is missing in the valence-band density of states for the amorphous cluster, which consists of two peaks, the lower one mostly *s*-like and the upper one mostly *p*-like. The *s*-like peak position is the same as its position in *c*-Si and its shape is preserved to a large extent. This suggests that the *s*-like eigenstates may still have a dispersion relation (in a spherically average sense) similar to that in the crystal[1] and that these states are less affected by disorder. A similar conclusion was reached by Kramer.[44] We show this in a more direct manner presently.

The *p*-like peak is shifted towards higher energy compared to its position in the crystal [see Fig. 5(a)]. We have already mentioned that the result for the crystalline cluster obtained via the recursion method also shows this shift because of a gradual departure from diamond-structure symmetry resulting from the accumulated errors of the higher recursion coefficients. In Fig. 5 we show a comparison of the density of states for the amorphous cluster with that of *c*-Si obtained via the **k**-space calculation. Here the shift in the *p*-band peak towards higher energy due to disorder can be clearly seen. The centroid of the *p* band shifts by ~ 0.5 eV toward the gap compared to that of the crystal. This is in reasonable agreement with the x-ray-photoelectron-spectroscopy (XPS) results of Ley *et al.*,[13] who found an 0.4-eV shift in the *p*-band peak position in *a*-Si.

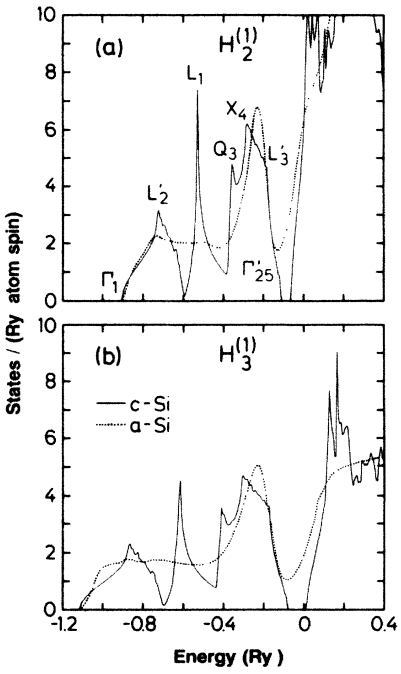

FIG. 5. Comparison of the density of states of *c*-Si obtained by the Brillouin-zone–summation method and of *a*-Si obtained by the recursion method using the Hamiltonians (a) $H_2^{(1)}$ and (b) $H_3^{(1)}$.

The valence-band spectrum of *a*-Si measured by XPS (Ref. 13) shows a double-peaked structure, but the relative heights of the two peaks are different from those in the electronic density of states we calculate. This is because of the difference in the matrix elements (photoelectron cross sections) involved in transitions from 3*s*-like as compared with 3*p*-like eigenstates [$\sigma(3s)/\sigma(3p) \approx 3.4$ in Si].[13] The results of our calculation [Fig. 5(a)] agree well with the experimental valence-band spectrum of *a*-Si after it has been corrected for variations in the photoelectron cross sections (Fig. 3.7b of Ref. 45), except that the L_2' and L_1 peak remnants are still distinguishable in the calculation and have not merged completely into one broad, flat hump as in the XPS spectrum.[45]

The calculated conduction-band density of states [Fig. 5(b)] compares similarly well with the x-ray-absorption spectra measured by Brown and Rustgi[12] and the partial-yield spectra of *a*-Si measured by Reichardt *et al.*[46] They found that the near-gap conduction band was completely structureless except for a 1.3-eV-wide hump at the conduction-band edge. The calculated conduction-band density of states is also completely structureless; there are no remnants of the critical-point structure of *c*-Si at the band edge. Ley[45] has argued that because electron-hole interactions are mostly responsible for the near-threshold enhancement of the partial-yield spectra of *a*-Si, the shape of the near-gap conduction band is best approximated by a simple step function. This assertion is supported by the results of our calculation and by recent bremsstrahlung-isochromat-spectroscopy results that show that the density of states varies smoothly above the conduction-band edge.[47]

Our calculation fails to produce a gap between the valence and conduction bands in *a*-Si. Because the recursion calculation for the *c*-Si cluster shows only a deep minimum instead of a true gap, the absence of a gap in the *a*-Si model can be partly attributed to the recursion method. A further reason for the relatively large density of states in the gap could be the approximate treatment of the interstitial region in the present electronic-structure calculation. We suggest some ways of improving this treatment in the next section. Finally, it cannot be excluded that our structural model for *a*-Si has states in the gap.

Hickey and Morgan[16] have calculated the electronic density of states for a similar model of *a*-Si, which they refer to as the WWW2 structure, using a model local pseudopotential. A comparison of their results with the density of states calculated for *c*-Si by Chelikowsky and Cohen[48] using the same local pseudopotential shows no relative shift of the *a*-Si *p*-band peak towards the gap. Furthermore, the height of the *a*-Si *p*-band peak in their

calculation is smaller than that for c-Si. In our calculation the a-Si p-like band becomes narrower and higher. Also, Hickey and Morgan[16] find a rather deep minimum (a pseudogap as in c-Si) between the s-like (L_2') states at the bottom of the valence band and the higher s-p (L_1) states. There is a very shallow minimum between these peaks in our results [Fig. 5(a)], but not nearly as pronounced. Because the structural models (especially the WWW2 model) studied by Hickey and Morgan and ourselves are essentially the same, the discrepancies in the respective results might be due to the model pseudopotential used in their calculations.

A qualitative description of the above-mentioned differences in the electronic density of states of a-Si and c-Si in terms of local disorder has been attempted.[3,7–9,45] It has been suggested that the shift in the p-band peak is primarily due to bond-angle variations,[45] but that near-gap p-band states are also sensitive to dihedral angle disorder.[8,9] The changes in the region of the L_2' and L_1 peaks are usually associated with topological disorder;[3] the presence of oddfold rings in the network introduces states between the main L_2 and L_1 peaks and results in a filling up of the gaps between them. The a-Si model contains bond-angle variations, dihedral angle variations, and oddfold rings. If these structural features are indeed directly responsible for characteristic features of the a-Si electronic density of states, we might expect to observe some correlation of the local densities of states of particular atoms in the a-Si model with the surrounding local structure.

C. Local densities of states

We have examined more than 50 local densities of states in order to determine the origin of their particular spectral features. In Fig. 6 we show some of these local densities of states for the Hamiltonian $H_2^{(1)}$, obtained by projection onto the orbitals of eight silicon spheres near the center of the cluster. For comparison we present in Fig. 7 the local density of states projected onto a silicon sphere in c-Si along with the s, p, and d projections. There is substantial variation in the a-Si local densities of states of the atoms presumably due to differences in the local environment.

We have attempted to relate the variation in the local density of states with the local distortions from the ideal diamond structure surrounding the atoms. The mean bond length and bond angle and their rms deviations, the local ring statistics, and the charge deviation from the mean (see next subsection) associated with each of the eight silicon atoms whose local densities of states we consider here are given in Fig. 6. Particular features in the local density of states do not seem to be correlated in any obvious way with these distortions. One might expect, for example, that the s-p –bonding peak would be present only in locally crystalline (or nearly ideal tetrahedral) environments. But this is not the case, at least not for the eight atoms whose local densities of states are shown in Fig. 6.

It is important to ascertain to what extent the computational methodology is responsible for the absence of

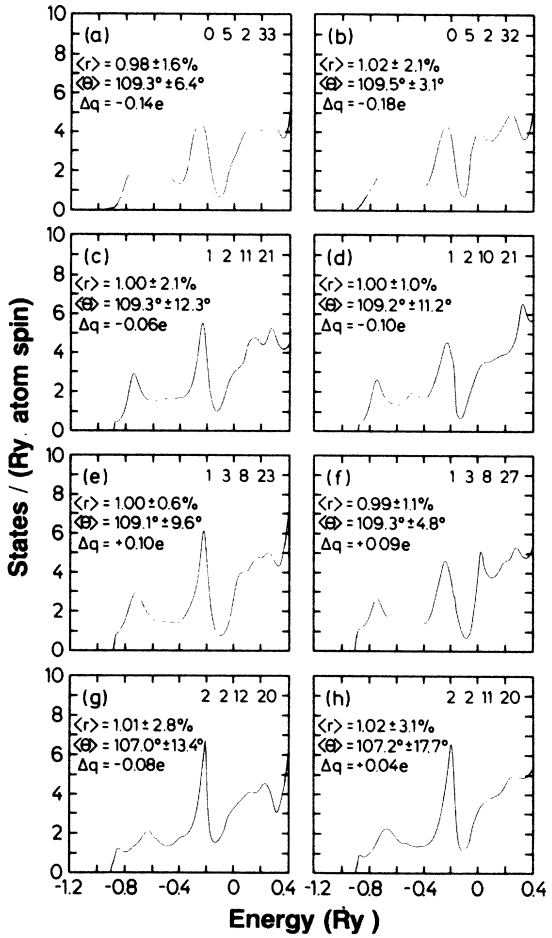

FIG. 6. Local densities of states for eight silicon spheres in the central region of the a-Si unit cell using the Hamiltonian $H_2^{(1)}$. The mean bond lengths and bond angles and their rms deviations, ring statistics (upper right-hand corner, five-, six-, seven-, and eightfold rings), and charge deviation from the mean for the corresponding atoms are also shown.

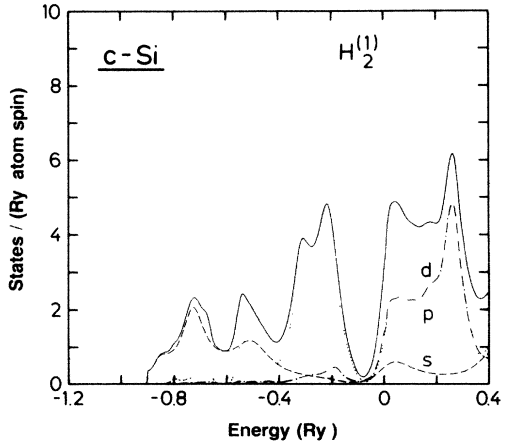

FIG. 7. Density of states projected onto a silicon sphere in c-Si obtained by using the recursion method in conjunction with the Hamiltonian $H_2^{(1)}$. The s, p, and d projections are also shown.

correlations between an atom's local bonding environment and particular features in its local density of states. We note that the same absence of correlations has been observed in a recent self-consistent TB LMTO recursion calculation of the electronic structure of a large (400 atoms) amorphous FeB cluster,[21] so that adding self-consistency to our computational prescription would probably not alter the situation to any significant degree. The improper treatment of the interstitial spheres, which might lead to the large density of gap states found in the *a*-Si calculation, might also be responsible for this absence of correlations. However, the fact that an average over the local *a*-Si densities of states agrees well with the experimental *a*-Si spectra suggests that the errors due to the method are small. In any case, differences in the local densities of states (and there are quite distinct differences, see Fig. 6) due to differences in the local environment should be less sensitive to the computational methodology because of the expected cancellation of errors. Therefore, we must look elsewhere for an explanation of the observed lack of correlations between local bonding environments and the local electronic densities of states.

The loss of long-range order in amorphous silicon, demonstrated by the lack of structure beyond about 10 Å in the pair-correlation function,[49] leads to the loss of **k** conservation normally required in its crystalline counterpart.[50] Calculations of the valence-band density of states[44] have shown that the loss of long-range order leads only to a slight broadening of the crystalline density of states. Because short-range order is basically preserved in *a*-Si, the remaining intermediate-range order should then to a large extent determine its electronic properties. We have mentioned the qualitative effects of dihedral angle disorder and the presence of oddfold rings on the valence-band density of states in *a*-Si, and that simple model calculations confirm these effects. It may therefore not be surprising that features in the calculated local densities of states are not correlated in any simple way with the local (short-range) geometric distortions surrounding the respective atoms. In particular, neither the width nor the position of the *p*-like band of states is correlated with the mean angle or its rms deviation. This raises some doubts about the interpretation of the *a*-Si *p*-band shift relative to its position in *c*-Si as due to the presence of bond-angle fluctuations in the amorphous network. These results suggest that, in general, correlations beyond nearest neighbors are important in determining the features in the valence-band density of states in *a*-Si.

Dihedral angle variations or the distribution of rings provide some measure of the intermediate-range correlations in an amorphous network. On the basis of simple model calculations, we might expect these measures to be linked in some manner to the origin of particular features in the electronic density of states of amorphous silicon. Because the dihedral angles in the *a*-Si structural model studied here are rather sharply distributed about their *c*-Si values,[15] deviations from the ideal diamond-structure ring statistics (i.e., the presence of oddfold rings) are the most likely determining structural distortions for the electronic density of states. However, we also find no clear correlation between the local ring statistics and the local densities of states (see Fig. 6). Atoms that are members of fivefold rings have local densities of states that are qualitatively indistinguishable from those of atoms that are members of no fivefold rings. Whether local topological distortions are correlated in any quantitative way with the subtle variations in the local valence-band densities of states or not remains unclear; we do not have a reliable way of quantifying the local topological environment surrounding atoms in an amorphous network. If there are indeed correlations between the local electronic properties and the local structure, there is no reason to expect that such correlations, which apparently must involve many atoms, will be simple functions of one physically intuitive variable.

D. Atomic charge distribution

We have calculated the total charge in 50 silicon spheres near the center of the *a*-Si cluster by integrating local densities of states up to the Fermi energy, and we find an average charge of 3.14 electrons per silicon sphere and 0.86 electrons per empty sphere. The rms charge fluctuation about the mean value for the silicon spheres is $0.14e$, in reasonable agreement with the experimentally measured value of $0.11e$.[51] Although the total charge in a given sphere depends on the sphere radius and thus is somewhat arbitrary, the calculated variation in this quantity should be a good measure of the charge fluctuation from one atom to another. For the purposes of comparison, the recursion-method calculation for *c*-Si with $H_2^{(1)}$ gives 3.18 electrons per Si atom and 0.82 electrons per empty sphere. Standard LMTO results for *c*-Si (Ref. 29) are 3.26 and 0.74, respectively.

Guttman, Ching, and Rath[52] calculated the electronic structure for several 54-atom network models of *a*-Si using the orthogonalized linear combination of atomic orbitals method. They also found a wide distribution of charges on the atoms (rms deviation from the mean $0.2e$) and attempted to relate the charge deviations to local geometric distortions in their models. They found that 60% of the calculated charge deviations could be accounted for by a simple function of first- and second-nearest-neighbor distances and suggested that correlations of four or more atoms might be required to account for the rest.

Winer and Cardona have shown that phenomenological models of charge transfer based on bond-length and bond-angle deviations from the ideal diamond structure are sufficient to account for the first-order infrared (ir) absorption in *a*-Si (Ref. 53) and the second-order ir absorption in *c*-Si (Ref. 54). One would intuitively expect that charge transfer in covalently bonded amorphous networks would depend to a large extent on short-range (geometric) structural distortions. The partial success of Guttman *et al.* in correlating charge fluctuations with geometric distortions, and the use of similar correlations to successfully describe the ir absorption in *a*-Si supports this expectation.

We have also attempted to correlate the deviations of the charges in the silicon spheres from the mean value

with the local geometry surrounding the corresponding silicon atoms (Fig. 6). The charge deviations from the mean show no obvious correlation with the average local bond length or average local bond angle surrounding the atoms. The absence of such correlations in the model may result from the lack of self-consistency in the calculation or from the use of interstitial spheres, which may lead to an unrealistic distribution of charges. However, we believe these effects to be minor. The absence of simple correlations between the local charges and the local structure is indicative of the dependence of the local electronic properties on the intermediate-range environment surrounding atoms in the network. Just as with particular features in the local densities of states, the amount of charge in an atomic sphere seems to be determined by the distribution of many surrounding atoms, which apparently precludes simple correlations with one or another physically intuitive variable. That such correlations are found in very small clusters with model Hamiltonians might be an artifact resulting from the lack of an intermediate-range environment in the corresponding structural models. Further investigation is needed to clarify the role of structural distortions in static charge-transfer processes in a-Si.

E. Spectral functions

Remnants of the crystalline E-$\mathbf{k}$ dispersion relations in a disordered phase can be studied with the help of spectral functions.[55] The projected density of states onto a traveling wave of the form

$$|u_L^{\mathbf{k}}\rangle = \sum_{\mathbf{R}} |\chi_{RL}\rangle e^{i\mathbf{k}\cdot\mathbf{R}} \tag{19}$$

can be computed by choosing Eq. (19) as the starting vector in the recursion method. We consider the basis orbitals centered on the silicon spheres only and compute, using the Hamiltonian $H_2^{(1)}$, the s- and p-state spectral functions defined as

$$\eta_s^{\mathbf{k}}(E) = -\frac{1}{\pi} \lim_{\varepsilon\to 0^+} \mathrm{Im}\langle u_s^{\mathbf{k}} | G(E-i\varepsilon) | u_s^{\mathbf{k}}\rangle , \tag{20a}$$

$$\eta_p^{\mathbf{k}}(E) = -\frac{1}{\pi} \lim_{\varepsilon\to 0^+} \mathrm{Im} \sum_{P=x,y,z} \langle u_p^{\mathbf{k}} | G(E-i\varepsilon) | u_p^{\mathbf{k}}\rangle . \tag{20b}$$

The difference between these functions and the momentum-energy spectral functions considered by Hickey and Morgan[16] (projected density of states on plane waves of wave vector $\mathbf{k}$) is discussed in Ref. 55. The existence of well-defined peaks in either of these spectral functions is the analogue of a crystal band structure.

Some care should be taken in the interpretation of $\mathbf{k}$. For a crystalline structure with more than one atom per cell, $\mathbf{k}$ does not correspond to a Bloch-wave vector; instead it is an arbitrary parameter determining the relative phases of the orbitals in the travelling wave of Eq. (19). However, for a crystalline structure with only one atom per primitive cell, it does correspond to a Bloch-wave vector. In Fig. 8(a) we show the s-state spectral function for the c-Si cluster for various values of $\mathbf{k}$ in the [001] direction with k_z varying from 0 to $4\pi/a_0$, where a_0 is the lattice constant for the diamond structure. We also show the relative phases of the nearest-neighbor orbitals for the two extreme values of $\mathbf{k}$. At $\mathbf{k}=(0,0,0)$ all orbitals in Eq. (19) appear with the same sign and the corresponding s-state spectral function exhibits a peak only at the bottom of the valence band (Γ_1 state); it has zero amplitude on the Γ_2' state in the conduction band. At $\mathbf{k}=(0,0,4\pi/a)$, the nearest-neighbor orbitals appear in Eq. (19) with opposite signs and the s-state spectral function shows a peak in the conduction band at the Γ_2' point. As $\mathbf{k}$ goes from (0,0,0) to $(0,0,4\pi/a_0)$, the spectra function picks up states with s character from the valence and conduction bands. In fact, a given $\mathbf{k}$ may or may not be a good quantum number. If it is, then the corresponding spectral function contains sharp peaks. A variation of the peak position with $\mathbf{k}$ indicates a dispersion relation, although it does not reproduce a band in any particular symmetry direction.

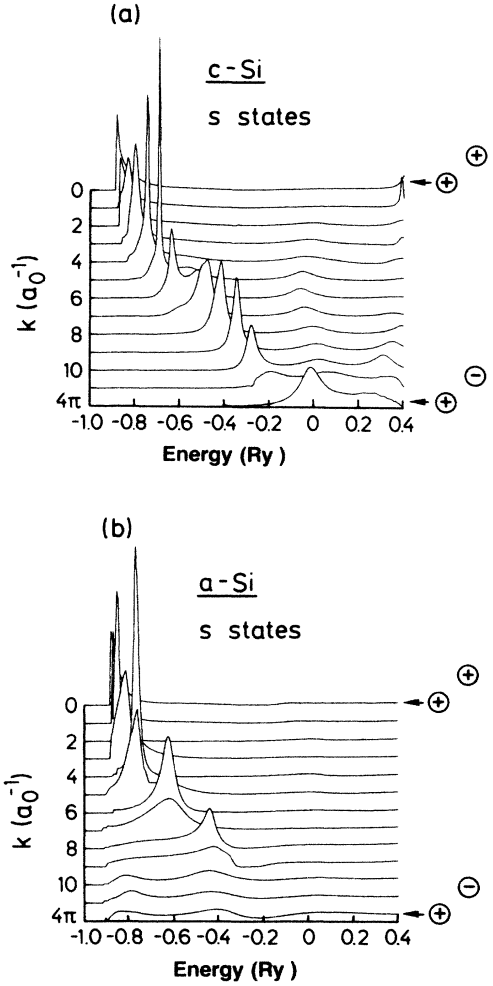

FIG. 8. Spectral functions for s states in (a) the c-Si cluster and (b) the a-Si model. The relative phases of the nearest-neighbor orbitals for the two extreme values of $\mathbf{k}$ are shown to the right of each figure.

In Fig. 8(b) we plot the s-state spectral functions for

the a-Si cluster for the same values of $\mathbf{k}$ as considered in Fig. 8(a). These results for the c-Si structure were calculated for a cluster of 855 sites (428 Si spheres, 427 empty spheres) with free boundary conditions. Because of the free surface the peaks in the corresponding spectral functions are somewhat broadened. For the a-Si structure we consider the 432-site cluster (216 Si spheres and 216 empty spheres) with periodic boundary conditions, thus minimizing finite-size effects. Any broadening in the peaks of the spectral functions for a-Si over that found for c-Si is thus mainly due to disorder and hybridization. It is clear that the s-state spectral functions for a-Si and c-Si show similar behavior from $\mathbf{k}=(0,0,0)$ up to almost $\mathbf{k}=(0,0,2\pi/a_0)$. Near $\mathbf{k}=(0,0,0)$ the s-state spectral functions for c-Si and a-Si are remarkably similar. This suggests that the lower part of the valence band, which is predominantly s-like, remains basically unaffected in the transition from the c-Si to the a-Si phase.

In Fig. 9 we show the p-state spectral functions. The $\mathbf{k}$ values considered are the same as in Fig. 8 and the relative phases of the nearest-neighbor p orbitals for the two extreme $\mathbf{k}$ values are also shown. At $\mathbf{k}=(0,0,0)$ the p-state spectral function has zero amplitude on the Γ'_{25} (top of the valence band) states and shows a peak at an energy corresponding to the Γ_{15} states (bottom of the conduction band). At $\mathbf{k}=(0,0,4\pi/a_0)$ states from the top of the valence band (Γ'_{25}) are picked up by the p-state spectral functions. This behavior is exhibited by both the c-Si and the a-Si p-state spectral functions. Near $\mathbf{k}=(0,0,4\pi/a_0)$ a subband structure in the p-state spectral function [see Fig. 9(a)] for the c-Si cluster can be seen. This subband structure is absent from the a-Si spectral functions. The different subbands seem to merge into one peak, which is somewhat broader than the main peak in the c-Si spectral function. As $\mathbf{k}$ goes from $(0,0,4\pi/a_0)$ to (0,0,0), the amplitude of the spectral function in the valence band decreases both for the a-Si and c-Si clusters and at $\mathbf{k}=(0,0,0)$ only the states with Γ_{15} symmetry in the conduction band are present.

Although the $\mathbf{k}$ values considered in the study of the spectral functions cannot be identified with the Bloch-wave vectors, it seems plausible to conclude that the s-like eigenstates in a-Si follow a dispersion relation similar to that in c-Si for a substantial range of $\mathbf{k}$ near $\mathbf{k}=\mathbf{0}$. The double-branched part of the p band appears as a simple broad peak in the p-state spectral functions. In short, the spectral functions in the disordered phase seem to exhibit the broadening behavior suggested by Ziman (see Fig. 8 of Ref. 1).

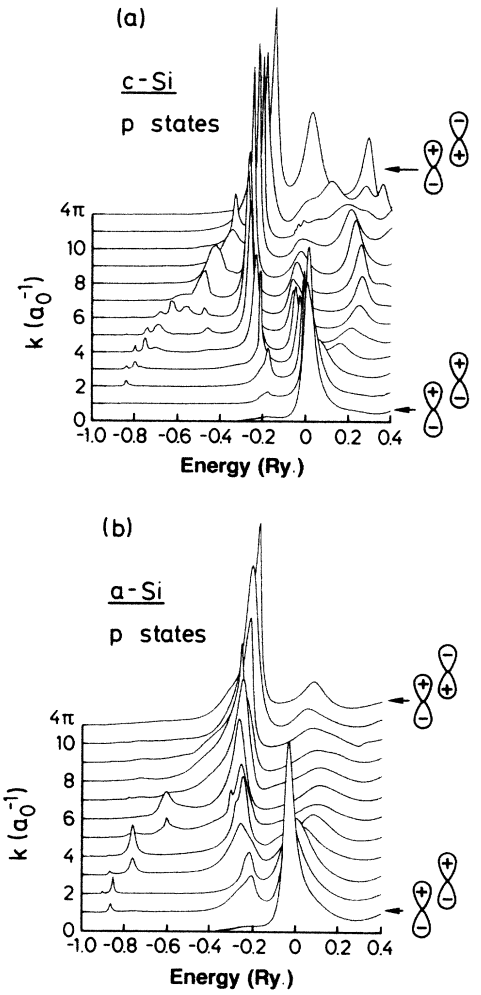

FIG. 9. Spectral functions for p states in (a) the c-Si cluster and (b) the a-Si model. The relative phases of the nearest-neighbor orbitals for the two extreme values of $\mathbf{k}$ are shown to the right of each figure.

V. CONCLUDING REMARKS

There are some weak points in the present electronic-structure calculation. Most of them concern our application of the two-center tight-binding Hamiltonian,

$$H^{(1)}_{RL,R'L'} \equiv c_{Rl}\delta_{RL,R'L'} + (d_{Rl})^{1/2} S_{RL,R'L'} (d_{R'l'})^{1/2} , \qquad (21)$$

in the open amorphous structure using the potential parameters c and d, which characterize the atomic- and interstitial-sphere potentials in *crystalline* Si. This approximation could, in principle, be responsible for the relatively large density of states found in the gap region.

Whereas the atomic-sphere approximation (ASA), upon which the Hamiltonian in Eq. (21) is based, works well for crystalline Si (and, for instance, yields a charge density identical to that obtained from full-potential linear-augmented-plane-wave calculations[24]), this is not necessarily so for amorphous Si, because there the interstitial regions are not as compact as in the crystal, and they are not all identical. In the a-Si model the deviations from sphericity could presumably be regarded as small, provided the interstitial regions were filled with spheres of variable size. Hence, if instead of using only one sphere size the radii of the interstitial and the atomic spheres were adjusted locally in the amorphous structure, large sphere overlaps could be avoided and the ASA could be quite accurate. So far we have not attempted to do so because a determination of local sphere size plus calculation of potential parameters for each sphere seemed tedious; we believe that the fluctuations of the on- and off-site elements of the structure matrix, S, are far more important than those of the potential parameters.

Another possibility for avoiding large overlaps of inter-

stitial spheres onto atomic ones is to include the so-called combined correction to the ASA.[19,21,23,27] With this correction the overlap integrals are evaluated exactly rather than as the sum of integrals over spheres, and the requirement that the spheres be "space filling" is no longer valid. The potential in the interstitial region is now described as a flat potential superposed onto spherical potentials whose spheres may be small. This approach has not yet been implemented for amorphous systems because the Hamiltonian for the recursion calculation is more complicated than Eq. (21).

Our electronic-structure calculation was not self-consistent for the amorphous system. The main difficulty underlying such a calculation is, again, that the potential varies locally from one sphere to another and the potential parameters have to be calculated separately for each sphere. This problem can be handled at various levels of approximation.[21] For amorphous metallic alloys current approximations amount to calculating the average potential for all spheres of the same type, or calculating the potential exactly for a relatively small number of spheres at the center of the cluster and using the average value for the rest. However, it is not obvious whether for a-Si any of these approximations offer a substantial improvement over the simplest treatment, which assumes the potential in the Si and interstitial spheres to be the same as in the corresponding crystalline structure. For a-Si a more relevant approximation would probably be to allow local rigid shifts of the Si and interstitial-sphere potentials; that is, to allow the on-site potential parameters c (and not merely the on-site elements of the structure matrix) to be site dependent. This leads to the problem of calculating Madelung shifts for a large amorphous cluster. The standard Ewald technique demands enormous computation times for this task.[43] Recently, an alternative method involving the "unscreening" of the TB structure matrix has been proposed,[21,23] but remains to be tested for large amorphous clusters.

Our calculations used a fairly large basis set consisting of the nine s, p, and d orbitals for both the Si and interstitial (E) sites. It is possible to reduce this set[56,21] at the expense of sacrificing the two-center Hamiltonian (21) for a "down-folded" one which contains three-center terms and/or the combined correction.[27] Such three-center terms also occur in the second-order Hamiltonian (14b) used in recursion calculations[57] in order to avoid slicing the energy range into narrow panels as done in first-order calculations. A minimal TB basis set for the valence band consists of the four Si s and p orbitals plus the E (empty-sphere) s orbital; the Si d partial waves should be treated explicitly in the Hamiltonian, i.e., through three-center terms, whereas the E p and d waves are most easily treated implicitly through the combined correction. For the conduction band we have seen that the Si d orbitals provide a substantial contribution to the density of states and, for this energy region, the Si d and preferably also the E p orbitals must be retained in the basis.[56] In order to describe accurately the partial waves not included in the basis, the corresponding screening constants α_{Rl} must be chosen to vanish and, as a consequence, smaller basis sets have longer range.[21,23] In a real-space calculation one would gain in terms of storage by having a smaller basis, but the longer range of the structure matrix might necessitate the use of a larger cluster, as well as more distant neighbor interactions. Thus, whereas in **k**-space (supercell) calculations a smaller basis set is of definite advantage, this is not necessarily true in recursion calculations.

The question as to what extent the high density of states found in the gap region results from our use of the recursion method, from our use of the TB LMTO ASA method, from our correction of the gap given by the local-density approximation, and from the structural model for a-Si, cannot be answered in the present paper. Conventional LMTO band-structure calculations for the model crystal with 216 atoms per cell are presently being performed in order to shed light on this question.[58]

In spite of the various approximations and simplifications, we believe that our first-principles calculation provides a fairly accurate description of the electronic properties of the a-Si model considered. In particular, our conclusion that an atom's local density of states is affected less by the short- and more by the intermediate-range topology than is usually assumed should be taken seriously. The same conclusion was recently reached from similar calculations for amorphous transition-metal alloys whose structures are closely packed.[21]

The agreement between the calculated total density of states and the available experimental results suggests that the structural model is a reasonably realistic representation of the bulk, homogeneous structure of a-Si. This model is therefore a worthy candidate for future studies of the effects of hydrogen incorporation, alloying, or doping on the vibrational and electronic properties of a-Si.

ACKNOWLEDGMENTS

We are grateful to H. J. Nowak for assistance with some of the computer programs and to P. Vargas for providing us with his version of the "linear predictor terminator." We thank N. E. Christensen for many helpful suggestions and for supplying the self-consistent Si- and interstitial-sphere potentials for c-Si. One of us (K.W.) thanks the Alexander von Humboldt–Stiftung for continuing support. Two of us (S.K.B. and K.W.) acknowledge the warm hospitality of the members of the Max-Planck-Institut für Festkörperforschung.

APPENDIX

The potential parameters c_{Rl}^{α} and d_{Rl}^{α} entering the first-order two-center tight-binding Hamiltonian (21) are calculated from the value and slope at the sphere boundary, $r=s_R$, of the normalized solution, $\Phi_{Rl}(r)$, of the radial Schrödinger equation at the energy $E_{\nu Rl}$ using the following relations:[21,23]

$$c^{\alpha}=E_{\nu}+s\Phi(s)^2\frac{[D(\Phi(s))+l+1][D_l^{\alpha}(s)-D(\Phi(s))]}{D_l^{\alpha}(s)+l+1} \tag{A1}$$

and

$$(d^\alpha)^{1/2}=(s/w)^{l+1/2}(s/2)^{1/2}\Phi(s)\frac{D_l^\alpha(s)-D(\Phi(s))}{D_l^\alpha(s)+l+1}\ . \tag{A2}$$

Here and in the following we have dropped the subscripts Rl, and

$$D(\Phi(s))\equiv\left.\frac{\partial \ln|\Phi(r)|}{\partial \ln r}\right|_s \tag{A3}$$

is the radial logarithmic derivative of Φ, whereas

$$D_l^\alpha(s)\equiv D((s/w)^{-l-1}-(s/w)^l\alpha_l/[2(2l+1)]) \tag{A4}$$

is the radial logarithmic derivative of the tail expansion of the envelope function K^α. With all spheres of the same size, $s_R\equiv w$, and with the values in Eq. (4) for the screening parameters we have

$$D_l^\alpha(s)=2.3,\ 2.4,\ 2.6,\ \text{and}\ l\ , \tag{A5}$$

for $l=0,1,2$ and $l>2$, respectively. It is the existence of a Wronskian relation between $\Phi(r)$ and $\dot\Phi(r)$ which makes it possible to evaluate the two-center, first-order Hamiltonian without calculation of $\dot\Phi(r)$.

The third potential parameter, the radial overlap, o_{Rl}^α, depends on the radial logarithmic derivative of $\dot\Phi(r)$, and it may be obtained from

$$o^\alpha=\left[s\Phi(s)^2\frac{[D(\Phi(s))-D_l^\alpha(s)][D(\dot\Phi(s))-D(\Phi(s))]}{D(\dot\Phi(s))-D_l^\alpha(s)}\right]^{-1}. \tag{A6}$$

The standard[19,21–25] potential parameters, $C\equiv c^\gamma$, $\Delta\equiv d^\gamma$, and γ, are those of the two-center Hamiltonian in that special representation which is characterized by having vanishing radial overlaps, i.e., by having $o^\gamma\equiv 0$. This is the so-called nearly orthogonal representation, and the corresponding Hamiltonian is correct to second order and equals $H^{(2)}$ in Eq. (14a). The screening parameters, γ, are seen to be given by the condition that $D^\gamma(s)=D(\dot\Phi(s))$, and $C\equiv c^\gamma$ and $(\Delta)^{1/2}\equiv(d^\gamma)^{1/2}$ are then given by (A1) and (A2), respectively. Elimination of the values and slopes of $\Phi(r)$ and $\dot\Phi(r)$ yields the following relations between the potential parameters appropriate for the TB and the nearly orthogonal representations:

$$\frac{c^\alpha-E_\nu}{C-E_\nu}=\left[\frac{d^\alpha}{\Delta}\right]^{1/2}=\frac{1}{o^\alpha}\frac{\alpha-\gamma}{\Delta}=1+\frac{\alpha-\gamma}{\Delta}(C-E_\nu)\ . \tag{A7}$$

[1] J. M. Ziman, J. Phys. C **4**, 3129 (1971).
[2] D. Weaire, Phys. Rev. Lett. **26**, 1541 (1971).
[3] D. Weaire and M. F. Thorpe, Phys. Rev. B **4**, 2508 (1971); **4**, 3518 (1971).
[4] M. J. Kelly and D. W. Bullett, J. Non-Cryst. Solids **21**, 155 (1977).
[5] W. Y. Ching, C. C. Lin, and L. Guttman, Phys. Rev. B **16**, 5488 (1977).
[6] J. D. Joannopoulos and M. L. Cohen, Phys. Rev. B **7**, 2644 (1973).
[7] M. H. Cohen, J. Singh, and F. Yonezawa, J. Non-Cryst. Solids **35&36**, 55 (1980).
[8] F. Yonezawa and M. H. Cohen, in *Fundamental Physics of Amorphous Semiconductors*, edited by F. Yonezawa (Springer, Berlin, 1981), Vol. 25, p. 119.
[9] J. Singh, Phys. Rev. B **23**, 4156 (1981).
[10] J. D. Joannopoulos, Phys. Rev. B **16**, 2764 (1977).
[11] G. Wiech and E. Zöpf, in *Band Structure Spectroscopy in Metals and Alloys*, edited by D. J. Fabian and L. M. Watson (Academic, New York, 1973), p. 637.
[12] F. C. Brown and O. P. Rustgi, Phys. Rev. Lett. **28**, 497 (1972).
[13] L. Ley, S. Kowalczyk, R. Pollack, and D. A. Shirley, Phys. Rev. Lett. **29**, 1088 (1972).
[14] F. Wooten, K. Winer, and D. Weaire, Phys. Rev. Lett. **54**, 1392 (1985).
[15] K. Winer, Phys. Rev. B **35**, 2366 (1987).
[16] B. J. Hickey and G. J. Morgan, J. Phys. C **19**, 6195 (1986).
[17] See the articles by V. Heine, R. Haydock, and M. J. Kelly, in *Solid State Physics*, edited by F. Seitz and D. Turnbull (Academic, New York, 1980), Vol. 35.
[18] O. K. Andersen and O. Jepsen, Phys. Rev. Lett. **53**, 2571 (1984).
[19] O. K. Andersen, O. Jepsen, and D. Glötzel, in *Highlights of Condensed Matter Theory*, edited by F. Bassani, F. Fumi, and M. P. Tosi (North-Holland, Amsterdam, 1985), p. 59.
[20] T. Fujiwara, J. Non-Cryst. Solids **61&62**, 1039 (1984).
[21] H. J. Nowak, T. Fujiwara, O. K. Andersen, O. Jepsen, and P. Vargas (unpublished).
[22] H. L. Skriver, *The LMTO Method*, Vol. 41 of *Springer Series in Solid State Sciences* (Springer, Berlin, 1984), p. 100.
[23] O. K. Andersen, O. Jepsen, and M. Sob, in *Proceedings of the International School on Electronic Band Structure Calculations and Their Applications*, Vol. 283 of *Lecture Notes in Physics*, edited by M. Yussouff (Springer, Berlin, 1987), p. 1.
[24] O. K. Andersen, Z. Pawlowska, and O. Jepsen, Phys. Rev. B **34**, 5253 (1986).
[25] O. K. Andersen, in *The Electronic Structure of Complex Systems*, edited by P. Phariseau and W. M. Temmerman (Plenum, New York, 1984), p. 11.
[26] See, for example, F. Cryot-Lackmann and S. N. Khanna, in *Excitations in Disordered Systems* (Plenum, New York, 1982), p. 59, and references therein.
[27] M. Sob, O. Jepsen, and O. K. Andersen (unpublished).
[28] M. Sob, O. Jepsen, and O. K. Andersen, Z. Phys. Chem. (to be published).
[29] N. E. Christensen, Phys. Rev. B **32**, 6490 (1985).
[30] O. Jepsen and O. K. Andersen, Solid State Commun. **9**, 1763 (1971).
[31] For crystalline clusters the most convenient way to calculate $H^{(2)}$ is to use Eqs. (65) and (66) from Ref. 19.
[32] See, for example, J. B. Perdew and M. Levy, Phys. Rev. Lett. **51**, 1884 (1983); R. W. Godby, M. Schlüter, and L. J. Sham, Phys. Rev. Lett. **56**, 2415 (1986); it is argued that the band gap remains small even if the exact exchange-correlation potential V_{xc} in the Kohn-Sham density-functional theory is used because of the discontinuity in V_{xc} upon addition of an electron to the system.
[33] This is equivalent to putting a hard potential at the center of the spheres, which only effects s waves. This latter procedure has been used previously [N. E. Christensen, Phys. Rev. B **30**, 5753 (1984)] to adjust the gap in electronic-structure calculations of semiconductors.

[34]R. Haydock and C. M. M. Nex, J. Phys. C **18**, 2235 (1985).

[35]G. Allan, in *The Recursion Method and Its Applications,* Vol. 58 of *Springer Series in Solid State Sciences,* edited by D. G. Pettifor and D. L. Weaire (Springer, Berlin, 1985), p. 61.

[36]P. Vargas, J. Phys. C (to be published).

[37]See discussion by R. Haydock on p. 233, and by V. Heine on p. 76, of *Solid State Physics,* Ref. 17, on this point.

[38]This number is dependent on the matrices $\underline{Q}^{-1}\underline{H}$ or $\underline{Q}^{-1/2}\underline{H}\,\underline{Q}^{-1/2}$ used in the calculation.

[39]The peaks do not arise entirely from the bands at particular symmetry points. However, we use these points to identify the peaks following the notation of M. S. Methfessel, M. H. Boon, and F. M. Mueller, J. Phys. C **16**, L949 (1983). Note that the Q points occur between the L and W points. The band structure for this symmetry line has not been shown in Fig. 1. The peak corresponding to Q_3 in our notation is labeled $\bar{W}_2$ by some authors—see J. D. Joannopoulos and M. L. Cohen, in *Solid State Physics,* edited by H. Ehrenreich, F. Seitz, and D. Turnbull (Academic, New York, 1976), Vol. 31, p. 105.

[40]P. N. Keating, Phys. Rev. **145**, 637 (1966).

[41]N. Metropolis, A. Rosenbluth, M. Rosenbluth, A. Teller, and E. Teller, J. Chem. Phys. **21**, 1087 (1953).

[42]W. Weber, Phys. Rev. B **15**, 4789 (1977).

[43]K. Winer and F. Wooten, Comput. Phys. Commun. **34**, 67 (1984).

[44]B. Kramer, Phys. Status Solidi B **47**, 501 (1971).

[45]L. Ley, in *The Physics of Amorphous Hydrogenated Silicon II,* edited by J. D. Joannopoulos and G. Lucovsky (Springer, Berlin, 1984), p. 61, and references therein.

[46]J. Reichardt, L. Ley, and R. L. Johnson, J. Non-Cryst. Solids **59&60**, 329 (1983).

[47]W. B. Jackson, S. M. Kelso, C. C. Tsai, J. W. Allen, and S.-J. Oh, Phys. Rev. B **31**, 5187 (1985).

[48]J. R. Chelikowsky and M. L. Cohen, Phys. Rev. B **10**, 5095 (1974).

[49]G. Etherington, A. C. Wright, J. T. Wenzel, J. C. Dore, J. H. Clark, and R. N. Sinclair, J. Non-Cryst. Solids **48**, 265 (1983).

[50]F. Wooten and D. Weaire, J. Phys. C **19**, L411 (1986).

[51]L. Ley, J. Reichardt, and R. L. Johnson, Phys. Rev. Lett. **49**, 1664 (1982).

[52]L. Guttman, W. Y. Ching, and J. Rath, Phys. Rev. Lett. **44**, 1513 (1980).

[53]K. Winer and M. Cardona, Solid State Commun. **60**, 207 (1986).

[54]K. Winer and M. Cardona, Phys. Rev. B **35**, 8744 (1987).

[55]S. K. Bose, L. E. Ballentine, and J. E. Hammerberg, J. Phys. F **13**, 2089 (1983).

[56]W. R. L. Lambrecht and O. K. Andersen, Phys. Rev. B **34**, 2439 (1986).

[57]S. K. Bose, S. S. Jaswal, and O. K. Andersen (unpublished).

[58]D. Sokolovski, O. K. Andersen, and M. Methfessel (unpublished).